An X-band Inverse Class-F SiGe HBT Cascode Power Amplifier With Harmonic-tuned Output Transformer

Inchan Ju and John D. Cressler

School of Electrical and Computer Engineering, Georgia Institute of Technology
777 Atlantic Drive N.W., Atlanta, GA 30332-0250 USA

***Abstract* — This paper presents a highly efficient X-band inverse class-F SiGe HBT cascode power amplifier (PA) to overcome performance limitations imposed by device breakdown. Simultaneous fundamental and 2nd/3rd harmonic matching is achieved using an output transformer with an embedded capacitor at its center-tap, which enables inverse class-F operation. Use of a cascode topology with a low base impedance termination and minimum voltage-current waveform overlap extends the V_{CE} swing on the upper SiGe HBT in the cascode to beyond BV_{CBO}, boosting output power and power added efficiency (PAE). As proof of concept, the inverse class-F PA was implemented in 0.13-µm SiGe BiCMOS technology. Measured results show an output power of 25.8 dBm and 51.1% peak PAE at 10 GHz, when operated on a 3.0 V supply. To the authors' best knowledge, our work has the highest efficiency among all Si-based X-band PAs with comparable output power.**

***Index Terms* — BV_{CBO}, cascode, harmonic, heterojunction bipolar transistor (HBT), inverse class-F, power amplifier (PA), silicon-germanium (SiGe), transformer, X-band.**

I. Introduction

With rapid scaling in transistors, Si-based technologies are becoming an ideal platform for the development of phased array and wireless communication systems because of their low cost, high yield, and dense integration compared with their III-V compound counterparts.

Si-based PAs remain a bottleneck because it is a power-hungry and is required to generate Watt level output power in a typical transmit module. While SiGe HBTs provide good noise and linearity characteristics, it is more vulnerable to breakdown than III-V technologies due to the inherent low bandgap in SiGe, hindering Watt level PA design. Thus, continuing efforts has been made to achieve high output power via several techniques such as Wilkinson power combiners, transformers, and stacking multiple transistors in series [1][2][3]. However, the efficiency is still low and thus a large portion of the RF power will be dissipated as heat, which adversely affects the overall system performance. Switching mode PAs, mainly used at radio frequency for efficient power generation, has recently been expanding its domain to microwave and even to millimeter-wave applications. A class-E PA [5] showed the potential for efficient power amplification, but its output power and efficiency were significantly affected and degraded by a parasitic capacitance. Inverse class-D PAs [6] are not suitable for use in X-band since they require square pulse shaping at the input. Therefore, harmonic-tuned inverse class-F PAs represent a possible alternative for realizing highly efficient PAs at microwave and millimeter-wave bands [7].

This work presents an X-band highly efficient sub-Watt level inverse class-F SiGe HBT cascode PA. An output transformer is designed, not only as a power combiner, but as a simultaneous fundamental and 2nd/3rd harmonic matching network with a simple even-mode impedance synthesizer. The very low base impedance of a common-base (CB) SiGe HBT in a cascode allows operation beyond BV_{CBO}, increasing the output power and efficiency. The designed PA delivers 25.8 dBm output power with 51.1% peak PAE at 10 GHz.

II. Inverse Class-F PA Design

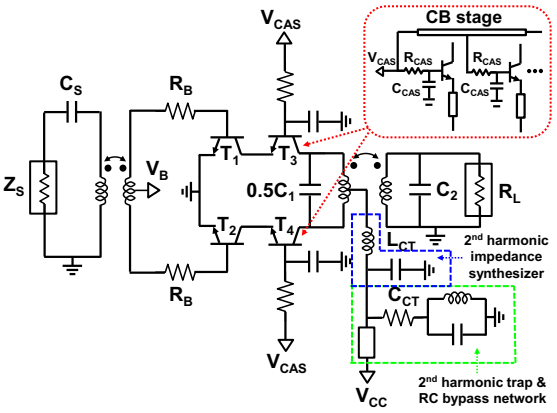

Fig. 1. Circuit schematic of the inverse class-F PA.

Fig. 1 shows a circuit schematic of the proposed X-band inverse class-F PA. A differential topology is adopted since it provides separate matching capability between odd- and even-modes, facilitating the optimization of fundamental

and 2nd harmonic impedance termination simultaneously. The PA consists of two cascode power cells with an input transformer balun and an output transformer. Both common emitter (CE) $T_{1,2}$ and CB $T_{3,4}$ are composed of 7 parallel CBE SiGe HBTs with emitter width and length of 0.12 µm and 17.8 µm, respectively. Each unit cell has a total emitter area of 14.95 µm^2, determined to reduce Kirk effect at high current density. Cascode breakdown heavily depends upon a base impedance termination and collector current density. A red dotted box in Fig. 1 reveals the detailed configuration of the CB transistor in cascode. The base of each SiGe HBT is terminated with a 1 pF dual-layered MIM capacitor C_{CAS} to bypass excessive holes generated by impact ionization. A series resistance R_B is used to broaden the bandwidth and stabilize the PA. A staggered-RC bypass network and a 2nd-harmonic trap [8] at the center-tap are introduced to suppress even-mode oscillation. Bias voltage at bases of CE and CB transistors, V_B and V_{CAS}, are 0.77 V and 1.5 V, respectively, for abrupt on/off switching of the SiGe HBTs.

III. Harmonic-Tuned Output Transformer

An output transformer matching network is depicted in Fig. 2. The output matching up to 3rd harmonic is realized by exploiting primary winding inductance variation and the different impedance seen at the transformer center-tap depending on mode of operation. A transformation ratio of 1:1 was chosen to convert a 50 Ω load to 25 Ω for each single-ended PA unit cell. The metal trace (AM) width and spacing between the adjacent turns of the output transformer are 20 and 3 µm, respectively. A patterned floating shield (M1) on the lossy Si substrate is used to raise its Q factor. The equivalent odd-mode half-circuit of the transformer is shown in Fig. 3 (a), which consists of an ideal transformer with a turn ratio of 1:(n/k), a shunt magnetizing inductance k^2L_{DM}, a series leakage inductance $(1-k^2)L_{DM}$, a parasitic capacitance C_P, and added capacitances C_1 and $2C_2$. The equivalent circuit can be further simplified by moving the load towards primary coil with proper impedance scaling, as shown in Fig. 3 (b). The matching procedure can be explained with the aid of the Smith chart, as shown in Fig. 5. The parallel k^2L_{DM} and $2(n/k)^2C_2$ is resonant at 10 GHz and thus Z_1 keeps the same location as R_{LT}. The series $(1-k^2)L_{DM}$ has Z_1 move to Z_2 and then the shunt capacitance C_1+C_P pulls Z_2 down to a Z_{OPT} of 25 Ω.

Fig. 4 indicates the equivalent even-mode half-circuit of the output transformer, where L_{CM} is the even-mode primary winding inductance. Due to the negative magnetic coupling from opposite current flows in the primary windings (red dotted arrow in Fig. 2), L_{CM} becomes smaller than L_{DM} and is related via the following equation.

$$L_{CM} = \left(\frac{1-k_P}{1+k_P}\right) \cdot L_{DM} \quad (1)$$

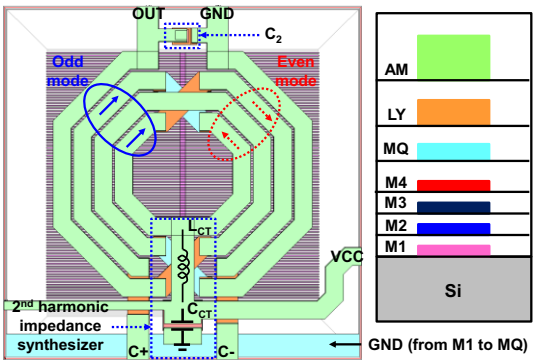

Fig. 2. A top view of the output transformer and a cross section of back-end-of-line (BEOL) metal stack.

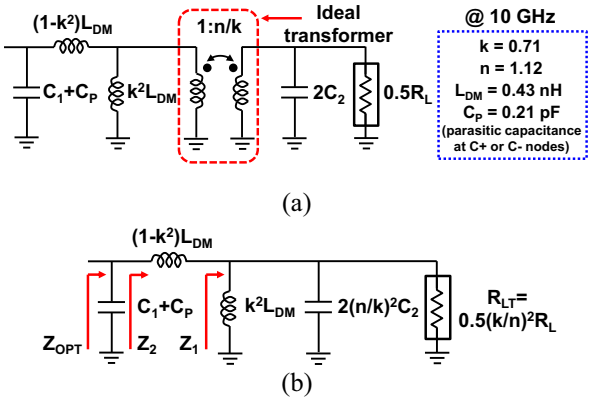

Fig. 3. The equivalent odd-mode half-circuit of the output transformer (a) with the leakage inductance shifted to the primary coil (b) all elements moved to the primary winding.

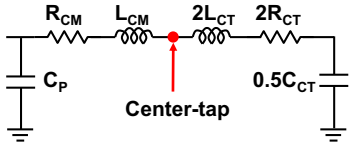

Fig. 4. The equivalent even-mode half-circuit of the output transformer.

where k_P is a self-magnetic coupling coefficient in primary winding. Here, k_P of 0.25 is obtained from SONNET EM simulation and the calculated L_{CM} is 0.26 nH at 20 GHz.

In order to synthesize an impedance seen at collectors of CB HBTs close to open, $L_{CM}+2L_{CT}$ should be resonated with C_P at 20 GHz. As a 2nd harmonic impedance synthesizer, a dual-layered MIM capacitor C_{CT} is embedded right below the center-tap of the transformer, as shown in Fig. 2. The embedded capacitor is AC ground at 20 GHz, which helps to resonate C_P and $L_{CM}+2L_{CT}$. Since the center-tap is a virtual-ground in odd-mode, the added capacitor has no impact on the fundamental matching. The simulated input impedance of even-mode half-circuit is presented in Fig. 5, on which the peak resistance of 250 Ω at 20 GHz is observed. 3rd harmonic matching is also realized thanks to the combination of C_P, C_1, and self-resonant frequency

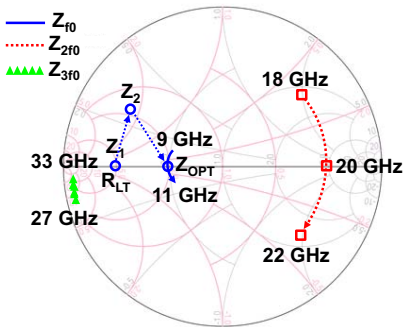

Fig. 5. Simulated fundamental, 2nd harmonic, and 3rd harmonic impedance loci seen at the collector of the PA unit cell.

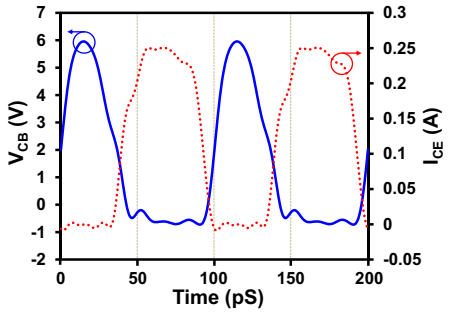

Fig. 6. Simulated transient waveforms of collector-base voltage (solid) and current source (dotted) for a CB SiGe HBT (P_{IN}=10-dBm at 10 GHz with 3.0 V supply).

nature of the transformer. The input balun is designed using a 2:1 inter-wined transformer [6] to transform the 50 Ω input to low impedance at the bases of the CE SiGe HBTs.

Time domain simulations of a collector-base voltage and a current source for the upper device in cascode are plotted in Fig. 6. The emitter current of the CB SiGe HBT is used as a first-order approximation of the inner current source I_{CE}. A half-wave rectified voltage and a quasi-square current waveform prove that the proposed output transformer successfully manipulates harmonic termination for inverse class-F operation. In addition, the minimum overlapping of the voltage-current waveforms would extend the V_{CB} swing above BV_{CBO} depending on the base resistance of a CB SiGe HBT, leading to an increase in the output power and PAE [9].

IV. Measurement Results

The highly efficient X-band inverse class-F PA is implemented in the Global Foundries 0.13-µm SiGe BiCMOS-8HP technology with f_{max}/f_T of 280/220 GHz. The breakdown voltages of BV_{CBO} and BV_{CEO} are 6.0 and 1.7 V, respectively. The BEOL features a 4-µm thick aluminum metal layer with a 3.6 fF/µm^2 high density low foot-print dual-layered MIM capacitor. The chip photograph is shown in Fig. 7 and its die size is 1.0 mm x 0.9 mm including bond pads.

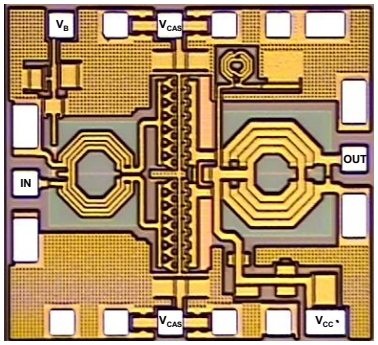

Fig. 7. A chip photograph of the inverse class-F PA.

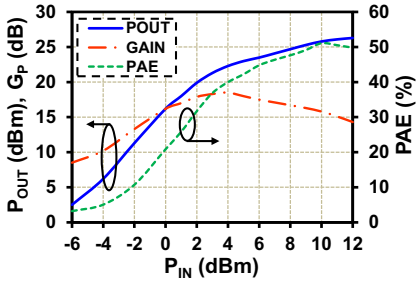

Fig. 8. Measured output power (P_{OUT}), PAE, and power gain (G_P) with the input power sweep at 10 GHz.

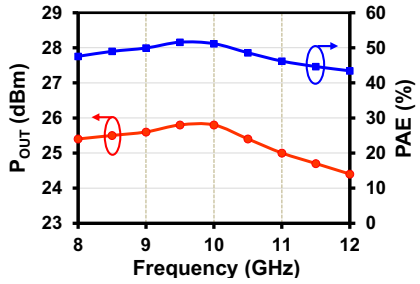

Fig. 9. Measured P_{OUT} and corresponding PAE over X-band.

The PA was characterized on wafer with a 3.0 V supply and a quiescent current of 5.2 mA. The output power, PAE, and power gain at 10 GHz are measured and those are shown in Fig. 8. The peak PAE is 51.1% with 25.8 dBm output power and 15.8 dB power gain at the input power of 10 dBm. The saturated output power is 26.3 dBm. The measured output power and PAE over X-band at the input power of 10 dBm are also depicted in Fig. 9. The output power is higher than 24.8 dBm and the PAE is better than 44.6% from 8.0 to 11.5 GHz, indicating a fractional 1-dB power gain bandwidth of 35%. Reliability testing was carried out with the setup as shown in Fig. 6. The output power and PAE are not degraded after 10 hours continuous mode, which proves the PA is robust to high voltage swing.

Finally, state-of-the-art performance among Si-based X-band PAs is summarized in Table I. Our work achieves the highest efficiency with comparable output power, and thus it should be an attractive candidate for the realization of highly integrated X-band phased array systems.

TABLE I
COMPARISON OF STATE-OF-THE-ART X-BAND PAS

Reference	[1]	[2]	[3]	[4]	**This Work**
Technology	130 nm SiGe	180 nm SiGe	90 nm CMOS	110 nm CMOS	**130 nm SiGe**
Class	AB	AB	AB	Harmonic-tuned	**Inverse class-F**
P_{SAT} (dBm)*	29.5	26.0	25.0	19.5	**26.3**
Peak PAE (%)*	17.8	35.0	20.0	25.0	**51.1**
GAIN (dB)*	27.7	22.0	19.0	6.5	**15.8**
BW (GHz)**	8.0-12.0	7.2-10.2	6.2-11.0	6.0-14.0	**8.0-11.5**
Area (mm^2)	2.66	0.95	0.70***	0.70	**0.90**

* P_{SAT}, peak PAE, and gain are obtained at 10 GHz.
** BW is defined as the frequency range of the power gain 1 dB lower than that at 10 GHz.
*** Only core area is included.

V. SUMMARY

A highly efficient X-band cascode inverse class-F PA fabricated in a 0.13-μm SiGe BiCMOS technology was presented. The harmonic-tuned output transformer with the 2nd harmonic impedance synthesizer is proposed to enable inverse class-F PA operation. Measurement results show that a peak PAE of 51.1% with 25.8 dBm output power at 10 GHz. The output power saturates at 26.3 dBm. The power gain bandwidth is from 8.0 to 11.5 GHz, covering most of X-band. To our best knowledge, this is the highest PAE X-band PA in any silicon-based technology reported to date.

ACKNOWLEDGEMENT

This work was partially funded by the Georgia Tech Research Institute and the Georgia Electronic Design Center at Georgia Tech. The authors are grateful to M. Mitchell, G. Hopkins, A. Cardoso, N. Lourenco, M. Oakley, and the Global Foundries SiGe team for their support and contributions.

REFERENCES

[1] C. Liu *et al.*, "An 890 mW Stacked Power Amplifier using SiGe HBTs for X-band Multifunctional Chips," in *Proc. IEEE ESSCIRC,* Sep. 2015, pp. 68-71.

[2] E. Harir and E. Socher, "0.5W X-Band SiGe PA With Integrated Double-Tuned Transformer," in *IEEE MTT-S International Microwave Symposium,* June, 2013, pp. 1–4.

[3] H. Wang, C. Sideris, and A. Hajimiri, "A CMOS Broadband Power Amplifier With a Transformer-Based High-Order Output Matching Network," *IEEE J. Solid-State Circuit,* vol. 45, no. 12, pp. 2709-2722, Dec. 2010.

[4] S. Park and S. Jeon, "Wideband harmonic-tuned CMOS power amplifier with 19.5 dBm output power and 22.6% PAE over entire X-band," *Electronics Letters,* vol. 51, no. 9, pp. 703-705, April 2015.

[5] K. Datta and H. Hashemi, "Performance Limits, Design and Implementation of mm-Wave SiGe HBT Class-E and Stacked Class-E Power Amplifiers," *IEEE J. Solid-State Circuit,* vol. 49, no. 10, pp. 2150-2171, Oct. 2014.

[6] D. Chowdhury, L. Ye, E. Alon, and A.M. Niknejad, "An Efficient Mixed-Signal 2.4-GHz Polar Power Amplifier in 65-nm CMOS Technology," *IEEE J. Solid-State Circuit,* vol. 46, no. 8, pp. 1796-1809, Aug. 2011.

[7] S.Y. Mortazavi and K.-J. Koh, "Integrated Inverse Class-F Silicon Power Amplifiers for High Power Efficiency at Microwave and mm-Wave," *IEEE J. Solid-State Circuit,* vol. 51, no. 10, pp. 2420-2434, Oct. 2016.

[8] A. Suarez, S. Jeon, and D. Rutledge, "Stability Analysis and Stabilization of Power Amplifier," *IEEE Microwave Magazine,* vol. 7, no. 5, pp. 51-65, Nov. 2006.

[9] M. Oakley, U. Raghunathan, B. Wier, P. Chakraborty, and J.D. Cressler, "Large-signal Reliability Analysis of SiGe HBT Cascode Driver Amplifier," *IEEE Tran. Electron Devices,* vol. 62, no. 5, pp. 1383-1389, May 2015.